The Cryosphere

Parameterization of atmosphere–surface exchange of CO_2 over sea ice

L. L. Sørensen[1,2], **B. Jensen**[1], **R. N. Glud**[2,3,5,6], **D. F. McGinnis**[3,5,7], **M. K. Sejr**[2,3], **J. Sievers**[1,2], **D. H. Søgaard**[3,5], **J.-L. Tison**[8], and **S. Rysgaard**[2,3,4]

[1]Department of Environmental Science, Aarhus University, Frederiksborgvej 399, 4000 Roskilde, Denmark
[2]Arctic Research Centre, Aarhus University, C.F. Møllers Alle 8, 8000 Aarhus, Denmark
[3]Greenland Climate Research Centre, c/o Greenland Institute of Natural Resources box 570, Nuuk, Greenland
[4]Centre for Earth Observation Science, CHR Faculty of Environment Earth and Resources, University of Manitoba, 499 Wallace Building Winnipeg, MB R3T 2N2, Canada
[5]University of Southern Denmark, NordCEE, Campusvej 55, 5230 Odense M, Denmark
[6]Scottish Marine Institute, Scottish Association of Marine Science, Oban, Scotland
[7]Helmholtz Centre for Ocean Research Kiel, GEOMAR, Wischhofstrasse 1–3, 24148 Kiel, Germany
[8]The Laboratoire de Glaciologie, the Université Libre de Bruxelles, Belgium

Correspondence to: L. L. Sørensen (lls@dmu.dk)

Abstract. We suggest the application of a flux parameterization commonly used over terrestrial areas for calculation of CO_2 fluxes over sea ice surfaces. The parameterization is based on resistance analogy. We present a concept for parameterization of the CO_2 fluxes over sea ice suggesting to use properties of the atmosphere and sea ice surface that can be measured or calculated on a routine basis. Parameters, which can be used in the conceptual model, are analysed based on data sampled from a seasonal fast-ice area, and the different variables influencing the exchange of CO_2 between the atmosphere and ice are discussed. We found the flux to be small during the late winter with fluxes in both directions. Not surprisingly we find that the resistance across the surface controls the fluxes and detailed knowledge of the brine volume and carbon chemistry within the brines as well as knowledge of snow cover and carbon chemistry in the ice are essential to estimate the partial pressure of pCO_2 and CO_2 flux. Further investigations of surface structure and snow cover and driving parameters such as heat flux, radiation, ice temperature and brine processes are required to adequately parameterize the surface resistance.

1 Introduction

The Nordic Seas represent an important area for oceanic CO_2 uptake and due to the high productivity their potential uptake rates range among the highest of the world's oceans (Takahashi et al., 2002; Takahashi et al., 2009). However, these high-latitude oceans are partly covered with sea ice, which has been considered to inhibit the gas exchange between the ocean and the atmosphere (Tison et al., 2002; Toggweiler et al., 2003). Recent studies show that the formation and melting of sea ice and the chemical processes in the sea ice itself play an important role for surface partial pressure of CO_2 (pCO_2) and thus the oceans capacity for taking up CO_2 in these regions (Papadimitriou et al., 2012; Rysgaard et al., 2007, 2009, 2012, 2013; Søgaard et al., 2013).

In the Arctic, the retreat of sea ice has affected the air–sea gas exchange, but to what extent the Arctic Ocean will remain a sink for atmospheric CO_2 in the future is debated (Parmentier et al., 2013). In shelf and coastal regions where primary production is high resulting in low surface pCO_2 during the ice-free summers, reduced ice cover is expected to temporarily increase uptake of atmospheric CO_2 (Bates and Mathis, 2009). Studies indicate that the uptake capacity of the Arctic Ocean for atmospheric CO_2 might be limited

as a result of surface warming and increased stratification (Cai et al., 2010; Else et al., 2013). Others have shown that chemical processes during ice formation and melting could be an important factor resulting in low surface pCO_2 levels during melting of sea ice in summer (Rysgaard et al., 2007; Rysgaard et al., 2012) and that reduced formation of sea ice could result in lowered uptake of CO_2. In addition to these studies addressing drivers of pCO_2 in ice-free surface water in summer, the understanding of gas fluxes across sea ice is improving. As mentioned, sea ice has been considered to hinder gas exchange between the ocean and the atmosphere (Tison et al., 2002; Toggweiler et al., 2003) and consequently no carbon cycle models have included CO_2 exchange through sea ice (Toggweiler et al., 2003). However, early studies by (Gosink et al., 1976) showed that sea ice can be permeable to gases including CO_2, especially at temperatures above $-7\,°C$. Furthermore, recent studies (Nomura et al., 2006; Nomura et al., 2010; Papadimitriou et al., 2004) suggest that formation of new ice leads to emission of CO_2 and that ice at higher temperatures is permeable and can take up atmospheric CO_2. Based on data from tank experiments, Nomura et al. (2006) suggest that 0.8 % of the total inorganic carbon (TCO_2) in sea water that becomes sea ice is emitted to the atmosphere during ice formation, resulting in a total emission of $0.04\,Gt\,C\,year^{-1}$ from ice formation in the Arctic and Antarctic. However, studies by Rysgaard et al. (2007) found that only a small amount (0.01 %) of CO_2 was released to the atmosphere. These findings suggest that oceans covered by sea ice can act as a source or a sink of atmospheric CO_2 depending on the concentration in the ice, which again is influenced by biogeochemistry, the thickness, the temperature and the permeability of the ice.

Until now only few studies have made an attempt to quantify the CO_2 ice–atmosphere flux over a larger area (local to regional scale) (Miller et al., 2011; Nomura, 2010; Papakyriakou, 2011; Semiletov et al., 2004; Zemmelink et al., 2006). Such assessments await a method for parameterization and upscaling of the CO_2 flux over sea ice as well as better knowledge of the CO_2 fluxes and the processes controlling these in order to estimate the atmospheric CO_2 dynamics in a future with changing sea ice cover.

Here we suggest applying the type of parameterizations, based on resistance theory (Hicks et al., 1987), commonly used for fluxes over terrestrial areas, to ice surfaces. We present a concept for parameterization of the CO_2 fluxes over sea ice suggesting using properties of the atmosphere and sea ice surface that can be measured or calculated on a routine basis. Parameters, which can be used in the conceptual model, are discussed based on data sampled from a seasonal fast ice area. This is to our knowledge the first attempt to parameterize air–sea ice fluxes of CO_2 using resistance theory.

2 Theory

The gas transfer between air and ice is in many ways similar to the transfer between terrestrial surfaces and air and to a lesser extent comparable to the transfer over an air–sea interface. The ice surface is not influenced by the atmospheric turbulence and does not change its surface physical characteristics with the wind on a short timescale as water does. However, this does not mean that wind is not an important parameter in driving the flux over ice. Air–surface exchange of gases is a consequence of the same atmospheric exchange mechanisms responsible for the surface fluxes of heat, moisture, and momentum, but is also strongly influenced by a range of surface properties (physical, chemical, and biological).

Surface exchange rates of trace gases can be measured by micrometeorological methods. The conservation equation provides the basic framework for measuring and interpreting micrometeorological flux measurements. In concept, the conservation equations state that the time rate of change of the mixing ratio of a gas at a fixed point in space is balanced by the mean horizontal and vertical advection (I), by the mean horizontal and vertical divergence or convergence of the turbulent flux (II), by molecular diffusion (III) and by any source or sink (S). The conservation equation is expressed as

$$\frac{\partial \overline{c}}{\partial t} = -\overline{u_i}\frac{\partial \overline{c}}{\partial x_i} - \frac{\partial \overline{u_i'c'}}{\partial x_i} + D\frac{\partial^2 c}{\partial x_i^2} + S, \qquad (1)$$

$$\underset{\text{I}}{} \qquad \underset{\text{II}}{} \qquad \underset{\text{III}}{}$$

where c is the concentration; u_i is the wind velocity where i denotes the velocity components in the lateral (x, y) and vertical (z) directions; D is the molecular diffusion coefficient of the quantity c in air; S is a source (positive) or sink (negative) term and overbar and prime denote the time-averaged and fluctuating quantities, respectively. Assuming the surface is uniform and level, no sink or source term exists in the atmosphere above the surface and the concentration of the gas does not vary significantly with time over the measurement period; Eq. (1) reduces to

$$\frac{\partial \overline{w'c'}}{\partial z} = -D\frac{\partial^2 c}{\partial x_i^2}, \qquad (2)$$

where w is the vertical wind velocity. Molecular diffusion results from the motion of the molecules due to random thermal motion. In the atmosphere this term is usually negligible in comparison to turbulent transfer, and thus the integration of Eq. (2) with respect to height yields (Baldocchi et al., 1988)

$$\overline{w'c'} = -D\frac{\partial c}{\partial z}, \qquad (3)$$

implying that the turbulent flux is constant with height within the atmospheric surface boundary layer and equals the

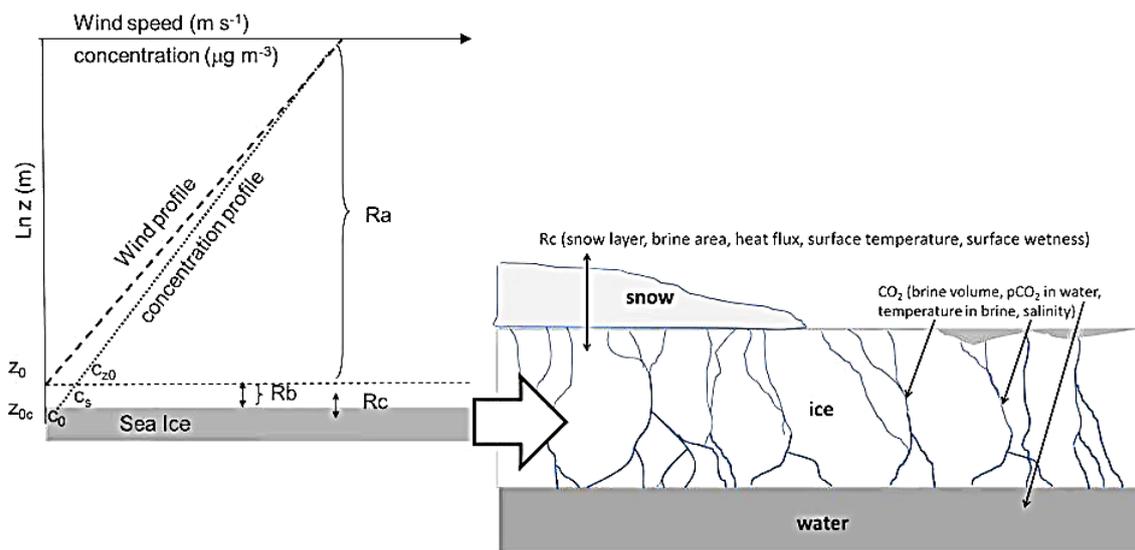**Fig. 1.** Left panel: Ra is the aerodynamic resistance over the layer dominated by atmospheric turbulence. Rb is the quasi-laminar boundary layer resistance over the layer, which is influenced by molecular diffusion and turbulence and Rc is the resistance over the ice/snow–atmosphere interface. The dashed line illustrates the logarithmic wind profile over the surface, which in theory goes to 0 at z_0. The dotted line illustrates the logarithmic concentration profile, which goes to the surface equilibrium concentration (c_s) at z_{0c}. Right panel: Sketch showing Rc and some of the parameters in/at the surface which Rc is affected by and $p\mathrm{CO}_2$ in the brine and parameters affecting this.

molecular gradient-diffusion flux at the surface. This also implies that fluxes measured using micrometeorological techniques (Businger, 1986; Businger and Delany, 1990; Fowler and Duyzer, 1989) at heights above the ground and fluxes measured by the enclosure techniques at the surface (Fowler et al., 2001) should be comparable. However, there are measurement issues that apply to all enclosure methods. Modification of the environment within the enclosure introduces many potential differences between the measured flux and that existing prior to the use of the enclosure. One of the largest uncertainties introduced using an enclosure (Fowler et al., 2001), even assuming that the effect of the enclosure on the environment and hence flux is negligible, is that of spatial variability in the flux. While chamber enclosures usually only integrate the signal over a few hundred square centimetres, exchange processes may be governed by controls that vary on scales of several hundred square metres (i.e. thickness and wetness of the snow cover, melt ponds, under-ice hydrology)

2.1 Surface exchange parameterization

The gas exchange between the surface and the atmosphere can be parameterized and evaluated in terms of resistances, which is understood as the resistance or limitation to the vertical transport between the atmosphere and the surface. The resistance accounts for the chemical, biological and physical processes that inhibit the transport. The resistance analogy has been used in deposition models since the 1980s (Hicks et al., 1987; Kramm et al., 1995; Kramm and Dlugi, 1994)

and is analogous to electrical current resistance. This model has two major resistance components (Hicks et al., 1987; Seinfeld and Pandis, 2012): (1) an aerodynamic resistance (Ra) that is wholly determined by physical atmospheric properties (predominantly turbulent exchange) and (2) a quasi-laminar boundary layer resistance (Rb) that accounts for the fact that gas transfer in the vicinity of the surface interface is affected by the molecular diffusivity. The resistance to transfer from the atmosphere is then $R = Ra + Rb$ and the flux F can be can be calculated as

$$\overline{w'c'} = F = -(c - c_s)\frac{1}{Ra + Rb}. \tag{4}$$

Where c is the concentration at the reference height and c_s is the concentration at the receiving surface. The resistances and the different layers are illustrated in Fig. 1. Ra is derived from the flux–gradient relationship. The vertical flux of trace gases above the surface can be expressed as the product of the eddy diffusivity (K) and the vertical concentration gradient $\partial c / \partial z$ based on the gradient transport theory (K theory). In practice, the concentration (and wind) profiles in the atmosphere are nearly log-linear (see Fig. 1) when the temperature gradient over the layer does not diverge from the adiabatic lapse rate (neutral stratification). The deviation from this shape is due to the effects of thermal stratification of the air close to the surface. These effects of the temperature structure of the boundary layer increase the rates of turbulent transfer in unstable conditions (temperature decreasing with increasing height) and decrease K when the surface is cooler than the air (usually nocturnal or winter conditions), in stable
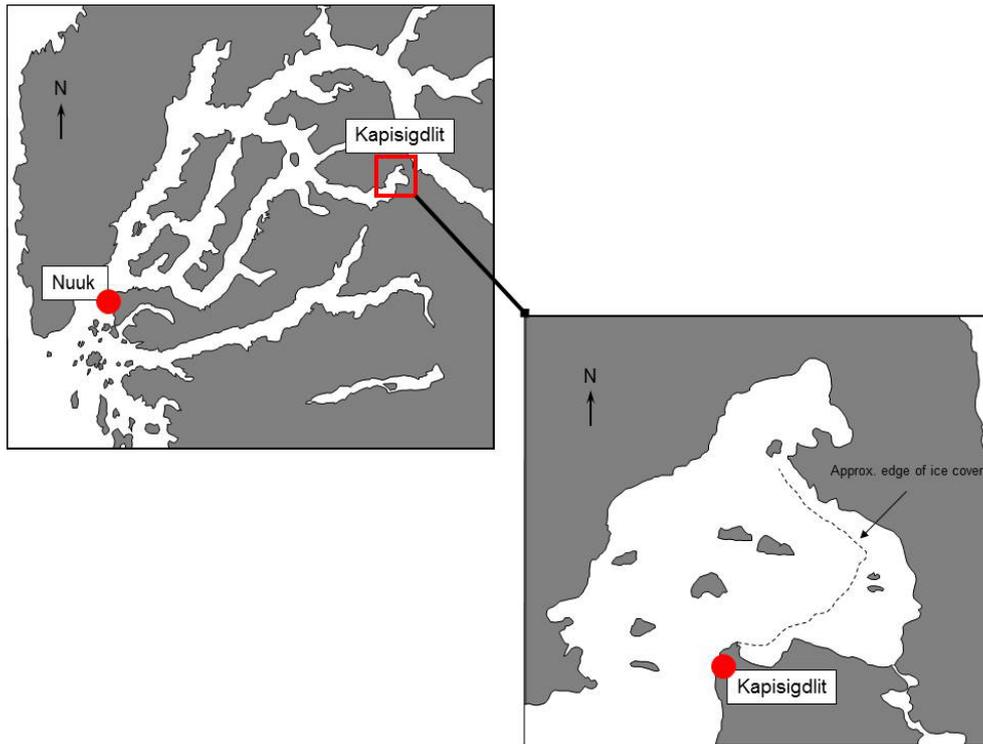
Fig. 2. Map showing the Nuuk fjord area in Greenland and the location of the field site near the town of Kapisigdlit ($64°26'10''$ N, $50°16'10''$ W).

conditions. The following parameterization for K is used for a neutral surface layer:

$$K = u_* \kappa z, \tag{5}$$

where u_* is the friction velocity, and κ is the von Karman constant (≈ 0.4). For the non-neutral surface layers (Hogstrom, 1996) a stability function φ is introduced (Businger et al., 1971); i.e.

$$K = \frac{u_* \kappa z}{\varphi\left(\frac{z}{L}\right)}, \tag{6}$$

where $\varphi(z/L)$ is the stability-dependent dimensionless concentration gradient. Following convention, stability is quantified in terms of z and the Obukhov length-scale L (Stull, 1988). Consider the flux of CO_2 with the local concentration gradient $\partial c/\partial z$ and following the methods of micrometeorology described above, the flux can be expressed in terms of the local vertical gradient of c as

$$F = -(u_* \kappa z) \frac{\partial c}{\partial z} \frac{1}{\varphi(z/L)}. \tag{7}$$

Rearranging and integrating over the turbulent layer between z and z_0, which is the familiar roughness length associated with momentum transfer estimated as the height where the logarithmic wind profile in theory becomes zero, leads to the form

$$c - c_{z_0} = -\frac{F}{\kappa u_*} \left[\ln \frac{z}{z_0} - \psi\left(\frac{z}{L}\right) \right], \tag{8}$$

where $\psi(z/L)$ is an integral form of the departure from neutral of the dimensionless concentration gradient and c_{z_0} is the concentration at the roughness height z_0. Ra is given by

$$Ra(z) = \frac{1}{\kappa u_*} \left[\ln \frac{z}{z_0} - \psi\left(\frac{z}{L}\right) \right]. \tag{9}$$

The second atmospheric resistance describes the resistance over the molecular turbulent sublayer, which is the layer between z_0 and the height z_{0c} where the concentration yields the equilibrium concentration with the surface (c_s). This resistance can thus be written in terms of z_0 and z_{0c}:

$$Rb = \frac{1}{\kappa u_*} \left[\ln \frac{z_0}{z_{0\,c}} \right]. \tag{10}$$

Modelling studies and wind-tunnel investigations confirm that Rb is strongly influenced by the diffusivity of the material being transferred. Effects associated with molecular or Brownian diffusivity lie outside the scope of the micrometeorological treatments leading to Eqs. (7), (8), and (9). However, specialized surface transfer models are available to deal with the problem (e.g. Brutsaert, 1975, 1979; Kramm, 1989;

Kramm et al., 1991; Kramm and Dlugi, 1994b). These models predict a functional dependence of Rb on the Schmidt number, i.e:

$$Rb = \frac{1}{u_*} \left[\frac{u_{z_0}}{u_*} + B_i^{-1} \right].$$ (11)

Where u_{z0} is a characteristic velocity for the layer $z_{0c} < z < z_0$ and B_i is the sublayer Stanton number, which is a function of the roughness Reynolds number and the Schmidt number ($Sc = \nu/Di$), with ν being the kinematic viscosity of air ($0.15\,\mathrm{cm}^2\,\mathrm{s}^{-1}$) and Di the molecular diffusivity of the gas i. However it is not a trivial task to obtain u_{z0}, since z_0 is estimated as the height were u becomes zero when extrapolating the logarithmic wind profile. Thus we use the more simple equation for Rb, which is suggested by Hicks et al. (1987) and used in many surface resistance models (Duyzer and Fowler, 1994; Spindler et al., 2001):

$$Rb = \frac{2}{\kappa u_*} \left(\frac{Sc}{Pr} \right)^{2/3},$$ (12)

where Pr is the Prandtl number for air (≈ 0.72).

A Rc is introduced to extend the resistance network analogy into the final receptor, corresponding to the stomatal compensation point model, often used for ammonia fluxes over terrestrial areas, treating bidirectional stomatal exchange driven by the difference between the atmospheric concentration c and the stomatal compensation point c_0 (Nemitz et al., 2001). In the case of sea ice c_0 is the equilibrium concentration in the brine. The flux for CO_2 can then be described in terms of resistances if Rc and the brine equilibrium concentration, c_0, is known.

The Rc and the Rb over ice surfaces have to our knowledge never been studied. If c_0 and the CO_2 flux can be estimated from measurements, Rc can be found from Eq. (13) assuming Rb can be calculated from Eq. (12):

$$\frac{(c - c_0)}{F} + (Ra + Rb) = -Rc.$$ (13)

3 Measurement of CO_2 fluxes

Measurements of CO_2, water vapour, temperature and vertical wind speed were conducted using fast sampling instruments (20 Hz) installed in a 3.5 m tower on an ice covered Greenlandic fjord close to the town of Kapisigdlit (Fig. 2) from 9 to 17 March, 2010. An open-path infrared gas analyser (LI-7500, LI-COR Inc., USA) was used for the measurements of CO_2 and water vapour and a USA-1 sonic anemometer (METEK GmbH, Germany) was used for measurements of the wind velocities in three dimensions and the fluctuation of atmospheric temperature. The thickness of the ice was 0.5–1 m and a 1–7 cm layer of snow covered it (Søgaard et al., 2013). Air temperatures were below 0 °C. A

small generator powered the equipment. To avoid contamination of the measurements from open water, snow scooter exhaust, or generators, we only use data from a limited fetch (wind direction 270–360° and 5–200°), which was not influenced by camp activities.

Air–ice fluxes of CO_2 were estimated using the same approach as Norman et al. (2012), where three different micrometeorological methods were applied. However, first the data set was filtered based on a careful inspection of spectra resulting in a set of data where the direction of the flux can be clearly identified from the cospectra and a clear similarity to calculated normalized spectra (Kaimal et al., 1972) is found (see Fig. 3). The eddy covariance (EC) technique, which is the basic micrometeorological method for flux estimation was then used as the primary method. Here, fluxes (F_γ) are derived from the covariance between the vertical velocity, w, and the concentration of the species of interest, γ (e.g. potential temperature, θ, water vapour or CO_2):

$$F_\gamma = \overline{w\gamma} + \overline{w'\gamma'}.$$ (14)

The first part of the flux is the vertical advection and the second term is the eddy correlation flux. The mean vertical advection is normally neglected because the vertical velocity is considered to be negligible, but when measuring CO_2 flux this term needs to be included since the difference in density between upward and downward moving air result in a non-negligible vertical velocity. This can be done by correction of the calculated fluxes (Webb et al., 1980) or the high frequent fluctuations (the raw signal) can be corrected (Sahlee et al., 2008). Here we use the approach by Sahlée (2008) since this will give a corrected time series, which is needed for spectral analysis. The EC technique is well known and widely used for atmospheric measurement of CO_2 fluxes (Baldocchi, 2003) over all types of surfaces.

Fluxes over sea ice are small and likely to be close to the detection limit. Wang et al. (2013), who used a similar instrumental setup over a cotton field, estimated the detection limit of CO_2 fluxes to be $1\,\mu\mathrm{g}\,\mathrm{C}\,\mathrm{m}^{-2}\,\mathrm{s}^{-1}$. These small fluxes are subject to dominance of errors introduced by, for example, sensor heating (Burba et al., 2008). Thus, to overcome some of the errors and obtain a more robust flux result we have used different frequency ranges of the turbulence spectrum for estimation of the fluxes.

In addition to the EC method, we have applied the inertial dissipation (ID) method, utilizing the high-frequency part of the spectra, and the cospectral peak (CSP) method, based on the lower frequencies. The ID method has traditionally been used to reduce the sensitivity to motion and flow distortion (Edson et al., 1991; Fairall and Larsen, 1986; Yelland and Taylor, 1996) for estimation of fluxes measured from moving platforms. However, here we use the ID method in addition to EC to ensure a higher confidence in the turbulent-flux estimate by using the high-frequency range of the turbulence spectrum. Using the ID method, the flux is determined with the aid of the normalized turbulent kinetic energy budget
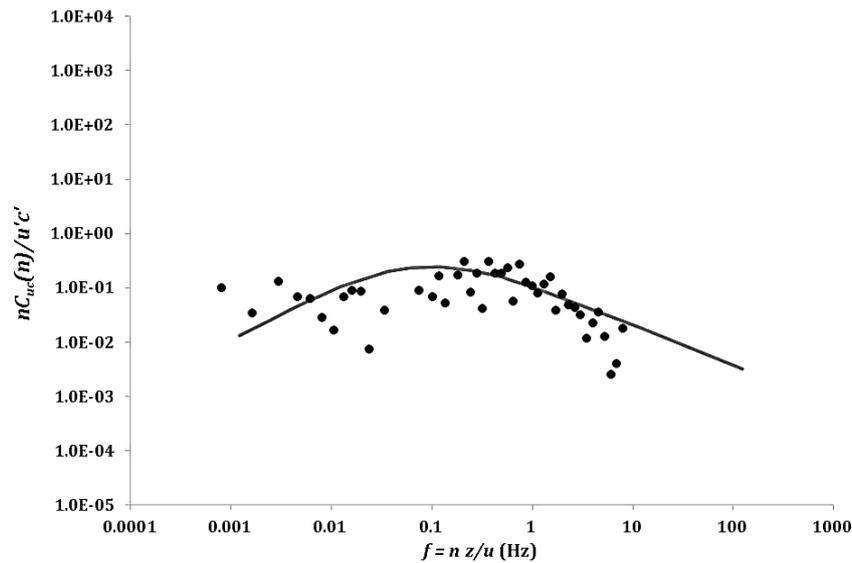
Fig. 3. Normalized logarithmic cospectra for CO_2 flux as a function of the normalized frequency (f), where n is the natural frequency, u is the wind speed and z the measurement height. The dots show the measured spectra and the solid line shows the calculated spectra for neutral conditions using the equation from Kaimal et al. (1972).

(Edson et al., 1991; Sjoblom and Smedman, 2004) assuming that the production of mechanical turbulence equals the molecular dissipation of the turbulent fluctuation. By using the ID technique, the inertial subrange of the power spectra is utilized for estimation of the flux. The ID technique is rarely used for measurements of CO_2 fluxes, however, it is shown by Sørensen and Larsen (2010) that it can be applied for CO_2 fluxes over water surfaces; and according to Sørensen and Larsen (2010) and Norman et al (2012) the ID method showed good agreement with the EC method. The application of the ID technique for CO_2 fluxes is only evaluated for neutral stratified atmospheric boundary layers, which makes the technique less reliable over ice, where the atmospheric stratification is usually very stable due to the cold surface. However, corrections based on scalar stability functions (Businger et al., 1971; Hill, 1989) for the stabilities encountered in this study were found to be small, thus we find it save to apply the stability corrections to the ID-estimated fluxes.

The basis for the CSP method is the existence of a universal spectrum for the cospectrum suggested by Kaimal et al. (1972). The full integral of the cospectrum yields the covariance, so if the spectral shape is universal and known, it is possible to derive the full integral from the integral over a limited spectral range. According to Sørensen and Larsen (2010) the flux can be estimated from the amplitude of the cospectrum multiplied by a constant that depends on the stability. The method recognizes relevant bell-shaped cospectra normalized with their fluxes tend to have their peak at the normalized frequency f (i.e. nh/u, where n is the natural frequency and h is the measurement height) between 0.01 and 0.2 with fairly broad maxima with an amplitude

maximum for a normalized cospectrum around 0.3 for momentum and 0.25 for a scalar at neutral conditions (Kaimal et al. 1972). The method was suggested from the observation that the cospectral bell-shape in the atmospheric surface layer is close to universal, with a slight systematic difference between momentum and scalars, from a number of measurement campaigns over land and water

Filtering data, based on spectral analysis and equality of the fluxes estimated by the three techniques, and on wind direction left 37 % of the original data for further analysis. The measured fluxes are shown in Fig. 4 as mean and standard deviation using three flux estimates for each sample. The measured CO_2 fluxes are in general small varying between -34 and $9\,\mu g\,C\,m^{-2}\,s^{-1}$ with a few incidents of upward fluxes but averaged over the sampling period the net flux is downwards ($-3\,\mu g\,C\,m^{-2}\,s^{-1}$). Only a single value is $< 1\,\mu g\,C\,m^{-2}\,s^{-1}$. The relative standard deviation on the estimated fluxes ranges between 1.3 and 220 % with an average of 76 %. Sørensen and Larsen (2010) found that for fluxes $< 60\,\mu g\,C\,m^{-2}\,s^{-1}$ the relative standard deviation exceeded 50 %. The standard deviations are relatively large; however we clearly see days with upward (March 12) and downward fluxes.

4   Estimation of the surface $p\text{CO}_2$

To estimate c_0, which is the partial pressure of CO_2 in the surface of the ice, measurements of temperature, total inorganic carbon (TCO_2), total alkalinity (TA), and salinity were carried out. Sea ice cores (of 9 cm diameter) were collected with a Mark II coring system (Kovacs Enterprises, Lebanon, NH). Vertical temperature profiles were measured
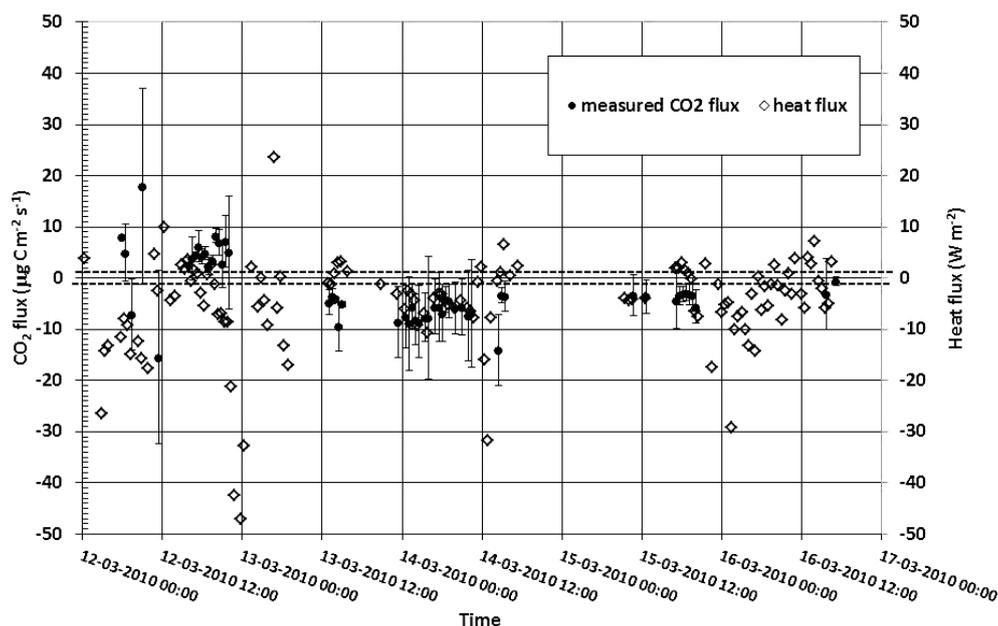
Fig. 4. Measured CO_2, and heat fluxes (Q) over the ice. The heat flux is measured using the eddy covariance (EC) technique and the CO_2 flux is estimated from EC technique, the cospectra peak method and the dissipation method. The dot shows the mean of the three methods and the bar shows the standard deviation.

Table 1. Average concentrations of bulk TCO_2 and TA and average sea ice bulk salinity. Data points represent data from 3 sampling days from the March 10 to 15, 2010.

Sea ice depth (cm)	Average bulk TCO_2 ($\mu mol\,kg^{-1}$)	Average bulk TA ($\mu mol\,kg^{-1}$)	Average bulk salinity (psu)
0	278 ± 14	312 ± 38	5.9 ± 0.6
12	202 ± 32	240 ± 68	7.6 ± 0.1
24	223 ± 58	265 ± 69	6.0 ± 0.3
36	238 ± 65	273 ± 98	5.9 ± 0.1
48	233 ± 64	331 ± 35	3.7 ± 0.5
60	283 ± 13	319 ± 20	6.3 ± 0.7

with a thermometer (Testo, Lenzkirch, Germany, and accuracy 0.1 °C) in the snow cover and in the sea ice at 12 cm intervals at the centre of the cores through 3 mm holes drilled immediately after coring. Each sea ice core was then cut into 12 cm sections, and each section transferred to a 1 L polyethylene jar and kept cold (insulated thermo box) until further processing within an hour in the ship's laboratory. In the laboratory, sea ice density was determined by shaping the ice core section into well-defined pieces with planar sides and then measuring the volume and weight of each segment. The segments were then cut in two. One half was melted within 2 h and 25 ml was collected for salinity measurements. The salinity of the melted sections (bulk salinity) was determined with a sonde (Knick Konduktometer, Germany) calibrated to a PORTASAL salinometer.

The other half of each sea ice section was used to determine TA and TCO_2 concentrations following Søgaard et al. (2013). Routine analysis of certified reference materials (provided by A. G. Dickson, Scripps Institution of Oceanography) verified that the accuracy of the TCO_2 and TA measurements was 0.5 and $2\,\mu mol\,kg^{-1}$, respectively. Ice samples were melted in gastight enclosures with aliquots of dilution water (artificial seawater) and bulk concentrations of TA and TCO_2 in sea ice (C_i) were calculated as described in Rysgaard and Glud (2004);

$$C_i = \frac{C_m W_m - C_a W_a}{W_i},\qquad(15)$$

where C_m is the TA or TCO_2 concentration in the mixture of melt and dilution water, W_m the weight of the melt water mixture, C_a the TA or TCO_2 concentration in the artificial seawater, W_a the weight of the artificial seawater, and W_i the weight of the sea ice. Average values are given in Table 1.

Temperatures in the ice surface were extracted from sensor array measurements performed at 30 min intervals during the
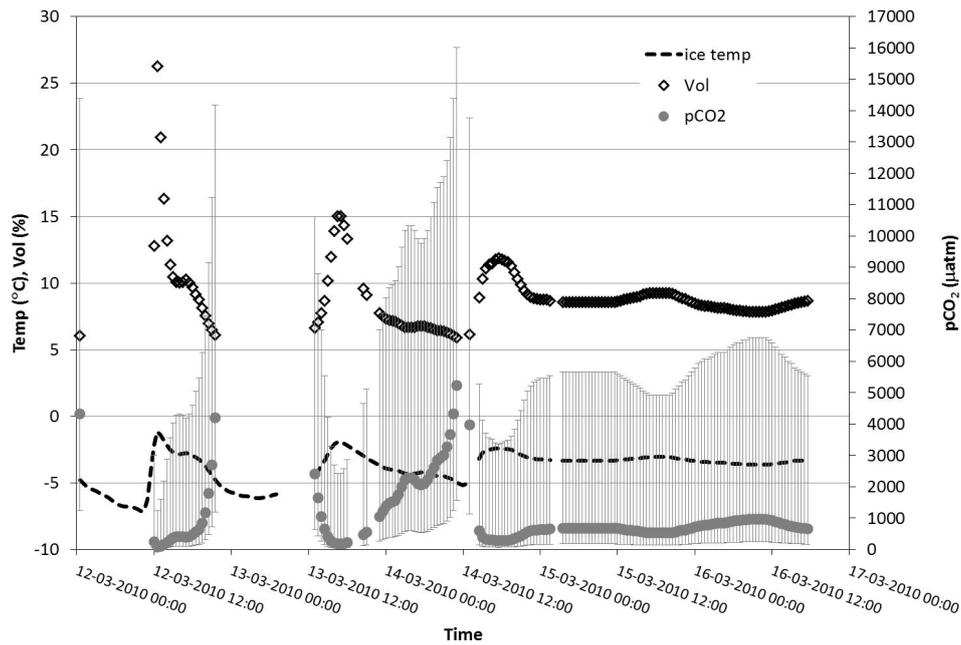
Fig. 5. Measured ice surface temperature (°C) and calculated brine volumes (%) and pCO_2 (µatm) in the brine channels from 12 to 16 March. The error bars around the pCO_2 are based on maximum and minimum values using the standard deviation on the measured salinity, TCO_2 and TA (see Table 1).

entire campaign. Essentially, custom built thermistors separated by a 4 cm distance were fixed on 3 m-long strings that were frozen into the ice as described in Jackson et al. (submitted). Here, we present the absolute surface values (Fig. 5), while the entire data set on ice, snow and water temperature profiles will be presented elsewhere.

Brine volume (Fig. 5) was calculated based on the temperature measured in the ice (Ti), the salinity measured in the ice (S_i) and the equation suggested by Timco and Weeks (2010):

$$B_{vol} = S_i \left(\frac{49.185}{|T_i|} \right) + 0.532. \tag{16}$$

For the measurement period, the following minimum and maximum values for the sea ice parameters were employed for calculations of pCO_2 in the ice surface: salinity 5.3–6.5, TCO_2 264–292 µmol kg^{-1}, TA 274–350 µmol kg^{-1}. The measured data are shown in Table 1. The partial pressure of CO_2 in the brine channels was estimated based on algorithms from Lewis and Wallace (1998) using dissociation constants from Goyet and Poisson (1989b) (temperature range from -1 to 40 °C and salinity range 1–50) due to low temperature and high salinity of the brine water. We are aware that salinity in the brines can exceed 50 when the brine volume becomes low, which adds uncertainty to the results at low temperatures and low volumes. When the brine volume was below 5 %, pCO_2 was not estimated as the ice is considered to be impermeable at these low brine volumes (Golden et al., 1998).

5 Calculation of *Ra*, *Rb* and *Rc*

In order to apply the resistance parameterization the resistances needs to be estimated. *Ra* and *Rb* are calculated from atmospheric parameters similar to the parameterization over terrestrial surfaces (Eqs. 9, 12). Using Eq. (13) and observed fluxes we calculate *Rc*, which, not surprisingly, is several orders of magnitude higher than *Ra* and *Rb*. In these stable atmospheric boundary layers *Ra* is large, however, it is clear that the resistance *Rc* across the surface must be even larger since the brine surface is limited and hence the transport across the surface is dominating and controlling the flux (Fig. 6).

However the *Rc* is varying and the parameters controlling *Rc* have to be estimated in order to be able to calculate *Rc* from routine measured parameters and apply the resistance model in larger-scale models. In the following section we will discuss some of these parameters.

6 Flux parameterization and discussion

To estimate the importance of sea ice for the uptake of CO_2, a parameterization of the transport across the surface is required and knowledge of the parameters driving this is fundamental. The parameterization of the atmospheric resistances is well known. However, it is also clear from the calculation of *Rc* from Eq. (13) that for this specific site and these specific climatic conditions *Rc* is the dominating resistance.
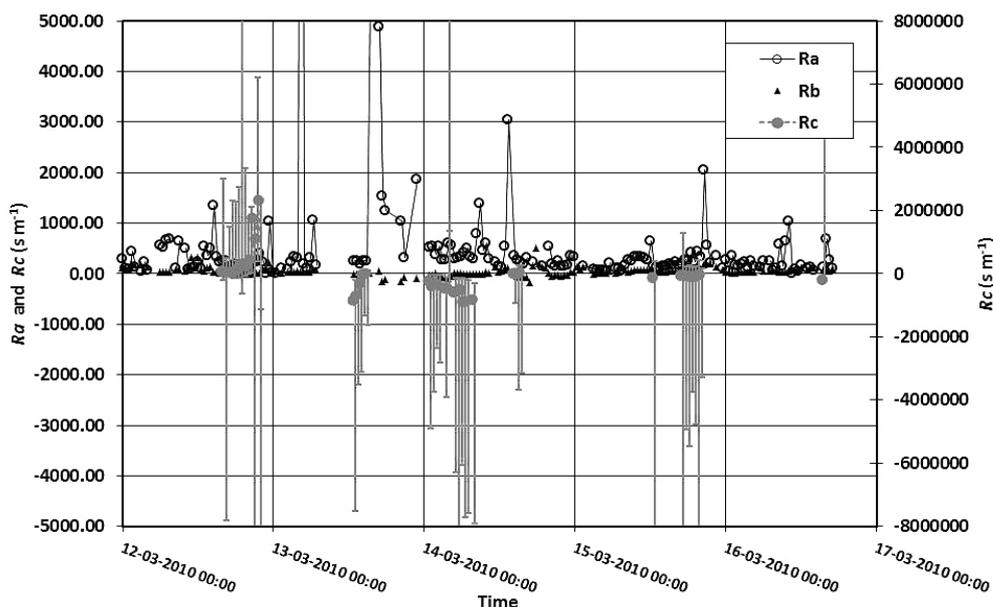
Fig. 6. Development of Rc, Ra and Rb from 12 to 16 March. The mean Ra is 5.24×10^2 s m^{-1} ranging from 0.05×10^2 to 236.32×10^2 s m^{-1} and mean Rb is 0.43×10^2 s m^{-1} ranging between 5.14×10^2 and -1.68×10^2 s m^{-1}. The Rc (mean -1.07×10^7 s m^{-1} ranging between 1.1×10^7 and -17.1×10^7 s m^{-1}) is several orders of magnitudes higher than Ra and Rb. The error bars around Rc are based on the calculated maximum and minimum values of pCO$_2$ in the surface brines.

Thus, an evaluation of the transfer mechanisms across the surface interface is essential.

For fluxes over terrestrial areas Rc can be estimated from simple parameterizations based on a constant resistant to complex parameterizations taking soil texture, surface wetness and leave stomatal opening or closure and processes within the stomatal into account (Duyzer and Fowler, 1994; Hicks et al., 1987; Sutton et al., 2001). The Rc for sea ice surfaces could be parameterized in a similar way using brine opening instead of stomatal opening and processes within the brine similar to processes within the stomatal. However in order to carry out a thorough analysis of Rc for sea ice and to suggest a complex parameterization, detailed information of the surface properties with a higher time resolution is needed. Nevertheless below we look in to some of the controlling parameters and suggest more detailed studies on these parameters in order to start developing a parameterization of Rc.

6.1 Parameters influencing the ice surface pCO$_2$

The flux magnitude and direction depends on the difference in pCO$_2$ between the brines and the overlaying atmosphere. We hypothesize that upward CO$_2$ fluxes from ice are associated with refreezing of brine channels leading to a decrease in brine volume, which again increases the brine pCO$_2$ levels in the ice surface. This is consistent with the measured CO$_2$ release coinciding with decreasing ice temperature on 12 March (Figs. 4, 5). But not consistent with the measurements on 14 March where we find clear downward fluxes at decreasing temperature and brine volume.
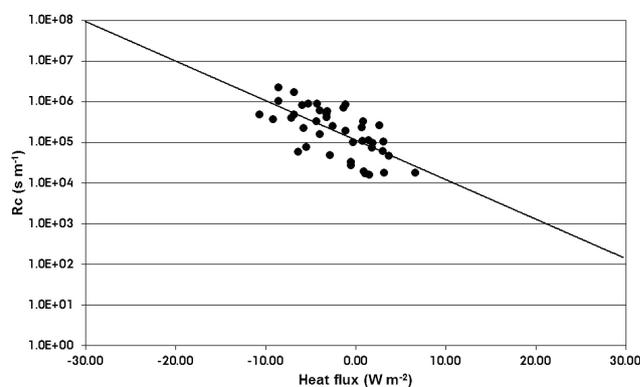

Fig. 7. The relation between the calculated Rc and the measured heat flux. The correlation coefficient R^2 is $\sim$0.5.

The pCO$_2$ on the ice surface varies both spatially and temporally depending on TA, TCO$_2$, brine volume, salinity and temperature of the ice. Therefore high precision TA and TCO$_2$ measurements as well as detailed knowledge of variations of temperature, brine volume and salinity are required to obtain a reliable pCO$_2$ estimate. Brine volumes were measured at different locations in our study area; however diurnal changes in air temperature, heat fluxes (Q) and solar radiation caused the surface temperature of the ice to vary by 1– 5 °C and have to be accounted for to realistically assess variations in pCO$_2$. In our study we assume that pCO$_2$ can be calculated using the algorithms in Lewis and Wallace (1998) from Goyet and Poisson (1989a), but these equations do not
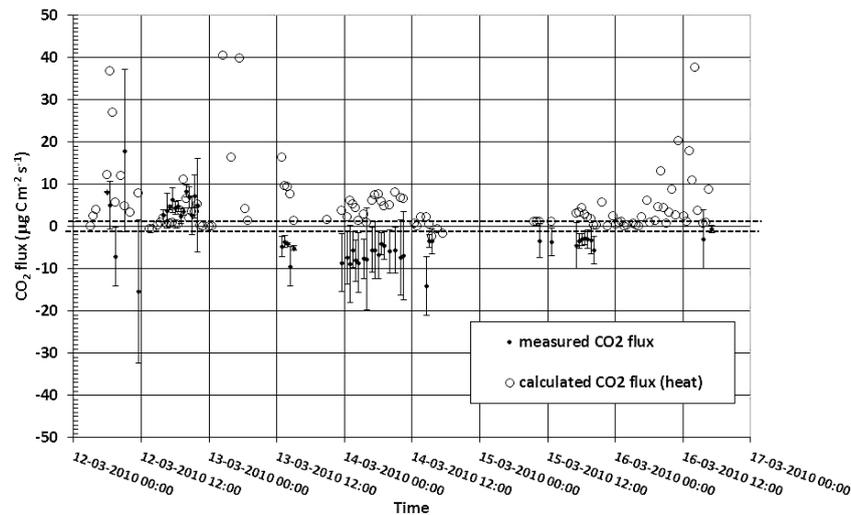
Fig. 8. The measured fluxes and the calculated fluxes using varying concentration based on brine volume calculated from ice temperature and Rc using the heat flux parameterization of Rc (o) as in Fig. 7. The CO_2 flux is estimated from EC technique, the cospectra peak method and the dissipation method. The dot shows the mean of the three methods and the bar shows the standard deviation.

take the formation of $CaCO_3$ in sea ice into account. Several studies suggest that the formation/dissolution of $CaCO_3$ affects the ice–atmosphere CO_2 flux (Geilfus et al., 2012; Søgaard et al., 2013). Søgaard et al. (2013) found formation of $CaCO_3$ in March 2010, in the surface ice in the fjord area by Kapisigdlit. During the formation of $CaCO_3$ CO_2 will be released, and dissolution of $CaCO_3$ will cause uptake of CO_2. It is possible that the upwards fluxes on 12 March are due to formation of $CaCO_3$ at decreasing temperatures and brine volumes and the downward heat fluxes on 14 March leads to dissolution of $CaCO_3$ and uptake of CO_2. These chemical reactions in the ice need to be investigated further in order to accurately estimate the pCO_2 in the brine.

6.2 Parameters influencing the surface exchange

The brine volume is not only influencing the pCO_2 but also the surface exchange, where small brine volume at low temperature results in small brine surface area. Thus one would expect decreasing Rc at decreasing temperature, which is found on 14 March. As illustrated in Fig. 1 the exchange over the surface is also influenced by the surface wetness and by the layer of snow on the ice surface. Variation in salinity, temperature and pCO_2 concentration in water or snow on the ice surface will affect the surface resistance. We did not observe water on the ice surface but as mentioned previously the ice was covered by snow. The temperature variation at the snow surface was not considered in the present study, however an ice crust on the snow surface was occasionally observed. Information about the thickness and structure of the snow cover as well as chemistry within the snow is important in order to properly evaluate Rc.

6.3 Discussion and parameterization of the surface resistance

The measured fluxes are small at low temperatures, likely due to low brine volume and thus small brine surface area, which makes it difficult to estimate the direction of the flux. This leads to large uncertainties in the calculated Rc, which we have found can even become negative. However the uncertainties of the calculated Rc is increasing at colder temperatures, which is due to measured small fluxes and an increasing difference between the atmospheric pCO_2 and the calculated brine pCO_2, where the largest uncertainty is due to lack of knowledge of the carbonate chemistry in sea ice. We have calculated pCO_2 based on Goyet and Poisson (1989), which is probably not adequate for calculation of pCO_2 in sea ice brines, since this does not take the formation of $CaCO_3$ in ice into account. Studies of sea ice and carbonate chemistry (Geilfus et al., 2012; Miller et al., 2011; Rysgaard et al., 2013; Søgaard et al., 2013) emphasize the importance of formation and dissolution of $CaCO_3$ on the levels of pCO_2 in the brines. An overestimation of pCO_2 is likely the explanation for the negative values of Rc.

We hypothesize that the heat flux between the ice and the atmosphere could be a parameter controlling the pCO_2 in the brines affecting both the $CaCO_3$ formation/dissolution and the brine volume. Therefore we investigate the correlation between the measured heat flux and the calculated surface resistance. Radiation was not measured but the magnitude of Rc aligns reasonably well to the measured heat flux (sensible plus latent) revealing an increase in Rc with increasing downward heat flux (Fig. 7). Potentially the correlation between heat flux and Rc could be confounded by the wind acting on the surface, which will result in a correlation with

the friction velocity (u_*) and, thus, indirectly a correlation to the heat flux. However, our data show no correlation between u_* and Rc (R^2 =0.04, p =0.16). The relation between Rc and heat flux shows increasing Rc with increasing downward heat flux. The downward heat fluxes can be initiated by very low surface temperatures which gives small brine area and thus high surface resistances. The heat flux is dominated by the sensible heat flux, which was primarily downward during the measurement period (mean heat flux = -8 W m^{-2}). However, this leads to an upward flux of the latent heat (mean heat flux = 2 W m^{-2}), which could explain the formation of an icy crust on the surface, possibly causing an increase in surface resistance. The surface resistance is calculated based on calculated pCO$_2$ brine values, which as mentioned is likely inadequate and thus the calculated Rc is highly uncertain. In order to calculate Rc and carry out a thorough test of controlling parameters the chemistry in the brine channels has to be well known.

Furthermore the surface exchange measured at our site will only be indirectly connected to the brine pCO$_2$ through the thin snow layer covering the ice. The vertical and lateral gas transport within the snow layer will control the pCO$_2$ on the surface (Liptzin et al., 2009; Massman and Frank, 2006). Nomura et al. (2010) found that the flux depends not only on the difference in pCO$_2$ between the brine and the overlying air but also on the condition of the sea ice surface and snow cover, especially during the ice-melting season. This indicates that measurements of the air–sea ice CO$_2$ flux should also include detailed observations of the sea ice's snow surface conditions. Not taking processes in the snow cover into account may also partly explain the negative Rcs.

Despite the large uncertainty on the calculated Rc we tested the parameterization of the CO$_2$ flux using the relationship, shown in Fig. 7, between the heat flux (Q) and Rc (Rc=163014e$^{-0.301Q}$) for parameterization of Rc. The fluxes were then calculated from Eq. (4) and compared to the measured flux (Fig. 8), which showed an average flux of $-2.6\,\mu$g C m^{-2} s^{-1} ranging between -34 and $8.7\,\mu$g C m^{-2} s^{-1}. The CO$_2$ flux, where Rc is based on a heat flux relation, shows mainly upward flux ranging from $-65\,\mu$g C m^{-2} s^{-1} to a few case of fluxes > 3000 μg m^{-2} s^{-1} and a mean flux of 954 μg m^{-2} s^{-1} (the computed flux is based on a calculated surface pCO$_2$ and a deficient Rc). As previously mentioned, the accuracy of the estimation of the pCO$_2$ on the surface is crucial, since this can even revise the direction of the flux.

The surface resistance is controlled by many parameters as illustrated in Fig. 1b and in order to carry out a thorough test of the relation between heating of the surface and the resistance method, measurements of radiation are required as well as detailed measurements of pCO$_2$ and physical-geochemical parameters of the ice and snow cover. As discussed in Sects. 6.1 and 6.2 the heat exchange between the atmosphere and the surface can influence both chemistry in the ice surface and the physical brine area. This can affect the

exchange and thus Rc in two different directions. Therefore it could be an approach to parameterize the surface exchange with a split of Rc in two parallel resistances describing the two processes similar to Nemitz et al. (2001).

7 Conclusions

The exchange of CO$_2$ between the atmosphere and the fast sea ice is ultimately driven by the difference of pCO$_2$ in the brines and the overlying atmosphere. We found the flux to be small (mean = $-3\,\mu$g C m^{-2} s^{-1}) during the late winter with fluxes in both directions. The flux is controlled by the pCO$_2$ in the surface brine which is controlled by the brine volume, surface temperature, TCO$_2$, TA and/or salinity. Furthermore, the chemistry of the carbonate system in the sea ice brine is essential to the brine pCO$_2$ and this chemistry is still poorly understood, thus it is not possible to accurately calculate pCO$_2$. We suggest a conceptual model for calculation of air–sea ice fluxes based on the resistance analogy, which is commonly used for terrestrial surfaces. We find that for our measurement site the surface resistance Rc is by far the largest and therefore the controlling resistance, and in order to calculate the fluxes from Eq. (4) a parameterization of Rc is needed. Such a parameterization requires detailed knowledge of the carbonate chemistry in the brine, the brine volume, TCO$_2$, TA and salinity as well as knowledge of snow cover and carbonate chemistry in the snow to estimate the accurate surface pCO$_2$. We believe that it is possible to measure fluxes over sea ice with a relative standard deviation of about 75 % in order to test the suggested parameterization, but the uncertainty of pCO$_2$ in the brine is too large. Further investigations of surface structure and snow cover on seasonal sea ice in parallel to measurements of driving parameters like heat flux, radiation, ice temperature and brine processes are required to parameterize Rc and to thoroughly test the resistance model for calculation of pCO$_2$ exchange over the air–sea ice interface in natural settings.

Edited by: T. R. Christensen

References

Baldocchi, D. D.: Assessing the eddy covariance technique for evaluating carbon dioxide exchange rates of ecosystems: past, present and future, Global Change Biol., 9, 479–492, 2003.

Baldocchi, D. D., Hincks, B. B., and Meyers, T. P.: Measuring Biosphere-Atmosphere Exchanges of Biologically Related Gases with Micrometeorological Methods, Ecology, 69, 1331–1340, 1988.

Bates, N. R. and Mathis, J. T.: The Arctic Ocean marine carbon cycle: evaluation of air-sea CO_2 exchanges, ocean acidification impacts and potential feedbacks, Biogeosciences, 6, 2433–2459, doi:10.5194/bg-6-2433-2009, 2009.

Brutsaert, W.: The Roughness Length for Water Vapor Sensible Heat, and Other Scalars, Journal of the Atmospheric Sciences, 32, 2028–2031, 1975.

Brutsaert, W.: Heat and mass transfer to and from surfaces with dense vegetation or similar permeable roughness, Bound.-Lay. Meteorol., 16, 365–388, 1979.

Burba, G. G., McDermitt, D. K., Grelle, A., Anderson, D. J., and Xu, L. K.: Addressing the influence of instrument surface heat exchange on the measurements of CO_2 flux from open-path gas analyzers, Global Change Biol., 14, 1854–1876, 2008.

Businger, J. A.: Evaluation of the Accuracy with Which Dry Deposition Can Be Measured with Current Micrometeorological Techniques, J. Climate Appl. Meteor., 25, 1100–1124, 1986.

Businger, J. A. and Delany, A. C.: Chemical Sensor Resolution Required for Measuring Surface Fluxes by 3 Common Micrometeorological Techniques, J. Atmos. Chem., 10, 399-410, 1990.

Businger, J. A., Wyngaard, J. C., Izumi, Y., and Bradley, E. F.: Flux-Profile Relationships in Atmospheric Surface Layer, J. Atmos. Sci., 28, 181–189, 1971.

Cai, W. J., Chen, L., Chen, B., Gao, Z., Lee, S. H., Chen, J., Pierrot, D., Sullivan, K., Wang, Y., Hu, X., Huang, W. J., Zhang, Y., Xu, S., Murata, A., Grebmeier, J. M., Jones, E. P., and Zhang, H.: Decrease in the CO_2 Uptake Capacity in an Ice-Free Arctic Ocean Basin, Science, 329, 556–559, 2010.

Duyzer, J. and Fowler, D.: Modeling Land Atmosphere Exchange of Gaseous Oxides of Nitrogen in Europe, Tellus B Chem. Phys. Meteorol., 46, 353–372, 1994.

Edson, J. B., Fairall, C. W., Mestayer, P. G., and Larsen, S. E.: A Study of the Inertial-Dissipation Method for Computing Air-Sea Fluxes, J. Geophys. Res.-Ocean., 96, 10689–10711, 1991.

Else, B. G. T., Galley, R. J., Lansard, B., Barber, D. G., Brown, K., Miller, L. A., Mucci, A., Papakyriakou, T. N., Tremblay, J. +., and Rysgaard, S.: Further observations of a decreasing atmospheric CO_2 uptake capacity in the Canada Basin (Arctic Ocean) due to sea ice loss, Geophys. Res. Lett., 40, 1132–1137, 2013.

Fairall, C. W. and Larsen, S. E.: Inertial-Dissipation Methods and Turbulent Fluxes at the Air-Ocean Interface, Bound.-Lay. Meteorol., 34, 287–301, 1986.

Fowler, D. and Duyzer, J. H.: Micrometeorological techniques for the measurement of trace gas exchange, in: Exchange of Trace Gases between Terrestrial Ecosystems and the Atmosphere, edited by: Andreae, M. O. and Schimel, D. S., John Wiley & Sons Ltd., Chichester, UK, 189–207, 1989.

Fowler, D., Coyle, M., Flechard, C., Hargreaves, K., Nemitz, E., Storeton-West, R., Sutton, M., and Erisman, J. W.: Advances in micrometeorological methods for the measurement and interpretation of gas and particle nitrogen fluxes, Plant Soil, 228, 117–129, 2001.

Geilfus, N. X., Carnat, G., Papakyriakou, T., TISON, J. L., Else, B., Thomas, H., Shadwick, E., and Delille, B.: Dynamics of pCO_2 and related air-ice CO_2 fluxes in the Arctic coastal zone (Amundsen Gulf, Beaufort Sea), J. Geophys. Res. Ocean., 117, C00G10, 2012.

Golden, K. M., Ackley, S. F., and Lytle, V. I.: The percolation phase transition in sea ice, Science, 282, 2238–2241, 1998.

Gosink, T. A., Pearson, J. G., and Kelley, J. J.: Gas movement through sea ice, Nature, 263, 41–42, 1976.

Goyet, C. and Poisson, A.: New Determination of Carbonic-Acid Dissociation-Constants in Seawater As A Function of Temperature and Salinity, Deep-Sea Research Part A-Oceanographic Research Papers, 36, 1635–1654, 1989a.

Goyet, C. and Poisson, A.: New determination of carbonic acid dissociation constants in seawater as a function of temperature and salinity, Deep Sea Res. Part A. Oceanogr. Res. Pap., 36, 1635–1654, 1989b.

Hicks, B. B., Baldocchi, D. D., Meyers, T. P., Hosker, R. P., and Matt, D. R.: A Preliminary Multiple Resistance Routine for Deriving Dry Deposition Velocities from Measured Quantities, Water Air Soil Poll., 36, 311–330, 1987.

Hill, R. J.: Implications of Monin−Obukhov Similarity Theory for Scalar Quantities, J. Atmos. Sci., 46, 2236-2244, 1989.

Hogstrom, U.: Review of some basic characteristics of the atmospheric surface layer, Bound.-Lay. Meteorol., 78, 215–246, 1996.

Kaimal, J. C., Wyngaard, J. C., Izumi, Y., and Coté, O. R.: Spectral characteristics of surface-layer turbulence, Q. J. R. Meteorol. Soc., 98, 563–589, 1972.

Kramm, G.: A numerical method for determining the dry deposition of atmospheric trace gases, Bound.-Lay. Meteorol., 48, 157–175, 1989.

Kramm, G. and Dlugi, R.: Modelling of the vertical fluxes of nitric acid, ammonia, and ammonium nitrate, J. Atmos. Chem., 18, 319–357, 1994.

Kramm, G., Dlugi, R., Dollard, G. J., Foken, T., Molders, N., Muller, H., Seiler, W., and Sievering, H.: On the Dry Deposition of Ozone and Reactive Nitrogen Species, Atmos. Environ., 29, 3209–3231, 1995.

Kramm, G., Muller, H., Fowler, D., Höfken, K. D., Meixner, F. X., and Schaller, E.: A modified profile method for determining the vertical fluxes of NO, NO_2, ozone, and HNO3 in the atmospheric surface layer, J. Atmos. Chem., 13, 265–288, 1991.

Liptzin, D., Williams, M., Helmig, D., Seok, B., Filippa, G., Chowanski, K., and Hueber, J.: Process-level controls on CO_2 fluxes from a seasonally snow-covered subalpine meadow soil, Niwot Ridge, Colorado, Biogeochemistry, 95, 151–166, 2009.

Massman, W. J. and Frank, J. M.: Advective transport of CO_2 in permeable media induced by atmospheric pressure fluctuations: 2. Observational evidence under snowpacks, Journal of Geophysical Research, 111, G03005, 2006.

Miller, L. A., Papakyriakou, T. N., Collins, R. E., Deming, J. W., Ehn, J. K., Macdonald, R. W., Mucci, A., Owens, O., Raudsepp, M., and Sutherland, N.: Carbon dynamics in sea ice: A winter flux time series, J. Geophys. Res. Ocean., 116, C02028, doi:10.1029/2009JC006058, 2011.

Nemitz, E., Milford, C., and Sutton, M. A.: A two-layer canopy compensation point model for describing bi-directional

biosphere-atmosphere exchange of ammonia, Q. J. Roy. Meteorol. Soc., 127, 815–833, 2001.

Nomura, D., Yoshikawa-Inoue, H., and Toyota, T.: The effect of sea-ice growth on air-sea CO$_2$ flux in a tank experiment, Tellus B Chem. Phys. Meteorol., 58, 418–426, 2006.

Nomura, D.: Effects of snow, snowmelting and refreezing processes on airГÇôsea-ice CO< SUB> 2< /SUB> flux, J. Glaciol., 56, 262-270, 2010.

Nomura, D., Yoshikawa-Inoue, H., Toyota, T., and Shirasawa, K.: Effects of snow, snowmelting and refreezing processes on airsea-ice CO$_2$ flux,

Norman, M., Rutgersson, A., Sorensen, L. L., and Sahlee, E.: Methods for Estimating Air-Sea Fluxes of CO$_2$ Using High-Frequency Measurements, Bound.-Lay. Meteorol., 144, 379–400, 2012.

Papadimitriou, S., Kennedy, H., Kattner, G., Dieckmann, G. S., and Thomas, D. N.: Experimental evidence for carbonate precipitation and CO$_2$ degassing during sea ice formation, Geochim. Cosmochim. Acta, 68, 1749–1761, 2004.

Papadimitriou, S., Kennedy, H., Norman, L., Kennedy, D. P., Dieckmann, G. S., and Thomas, D. N.: The effect of biological activity, CaCO$_3$ mineral dynamics, and CO$_2$ degassing in the inorganic carbon cycle in sea ice in late winter-early spring in the Weddell Sea, Antarctica, J. Geophys. Res.-Ocean., 117, C08011, doi:10.1029/2012JC008058, 2012.

Papakyriakou: Springtime CO< SUB> 2< /SUB> exchange over seasonal sea ice in the Canadian Arctic Archipelago, Ann. Glaciol., 52, 215–224, 2011.

Parmentier, F. J., Christensen, T. R., Sorensen, L. L., Rysgaard, S., McGuire, A. D., Miller, P. A., and Walker, D. A.: The impact of lower sea-ice extent on Arctic greenhouse-gas exchange, Nature Clim. Change, 3, 195–202, 2013.

Rysgaard, S., Bendtsen, J., Pedersen, L. T., Ramlov, H., and Glud, R. N.: Increased CO$_2$ uptake due to sea ice growth and decay in the Nordic Seas, J. Geophys. Res.-Ocean., 114, C09011, doi:10.1029/2008JC005088, 2009.

Rysgaard, S. and Glud, R. N.: Anaerobic N2 production in Arctic sea ice, Limnol. Oceanogr., 49, 86–94, 2004.

Rysgaard, S., Glud, R. N., Lennert, K., Cooper, M., Halden, N., Leakey, R. J. G., Hawthorne, F. C., and Barber, D.: Ikaite crystals in melting sea ice – implications for pCO$_2$ and pH levels in Arctic surface waters, Cryosphere, 6, 901–908, 2012.

Rysgaard, S., Glud, R. N., Sejr, M. K., Bendtsen, J., and Christensen, P. B.: Inorganic carbon transport during sea ice growth and decay: a carbon pump in polar seas, J. Geophys. Res., 112, C03016, doi:10.1029/2006JC003572, 2007.

Rysgaard, S., Søgaard, D. H., Cooper, M., Puc'ko, M., Lennert, K., Papakyriakou, T. N., Wang, F., Geilfus, N. X., Glud, R. N., Ehn, J., McGinnis, D. F., Attard, K., Sievers, J., Deming, J. W., and Barber, D.: Ikaite crystal distribution in winter sea ice and implications for CO$_2$ system dynamics, The Cryosphere, 7, 707–718, doi:10.5194/tc-7-707-2013, 2013.

Sahlee, E., Smedman, A. S., Rutgersson, A., and Hogstrom, U.: Spectra of CO$_2$ and water vapour in the marine atmospheric surface layer, Bound.-Lay. Meteorol., 126, 279-295, 2008.

Seinfeld, J. H. and Pandis, S. N.: Atmospheric Chemistry and Physics: From Air Pollution to Climate Change, John Wiley & Sons, 900–932, 2012.

Semiletov, I., Makshtas, A., Akasofu, S. I., and Andreas, E. L.: Atmospheric CO$_2$ balance: The role of Arctic sea ice, Geophys. Res. Lett., 31, L05121, doi:10.1029/2003GL017996, 2004.

Sjoblom, A. and Smedman, A. S.: Comparison between eddy-correlation and inertial dissipation methods in the marine atmospheric surface layer, Bound.-Lay. Meteorol., 110, 141–164, 2004.

Søgaard, D., Thomas, D., Rysgaard, S., Glud, R. N., Norman, L., Kaartokallio, H., Juul-Pedersen, T., and Geilfus, N. X.: The relative contributions of biological and abiotic processes to carbon dynamics in subarctic sea ice, Polar Biol., 36, 1761–1777, 2013.

Sørensen, L. L. and Larsen, S. E.: Atmosphere-Surface Fluxes of CO$_2$ using Spectral Techniques, Bound.-Lay. Meteorol., 136, 59–81, 2010.

Spindler, G., Teichmann, U., and Sutton, M. A.: Ammonia dry deposition over grassland – micrometeorological flux-gradient measurements and bidirectional flux calculations using an inferential model, Q. J. Roy. Meteorol. Soc., 127, 795–814, 2001.

Stull, R.: Turbulence Kinetic Energy, Stability and Scaling, An Introduction to Boundary Layer Meteorology, Kluwer Academic Publisher, 151–197, 1988.

Sutton, M. A., Milford, C., Nemitz, E., Theobald, M. R., Hill, P. W., Fowler, D., Schjoerring, J. K., Mattsson, M. E., Nielsen, K. H., Husted, S., Erisman, J. W., Otjes, R., Hensen, A., Mosquera, J., Cellier, P., Loubet, B., David, M., Genermont, S., Neftel, A., Blatter, A., Herrmann, B., Jones, S. K., Horvath, L., Fuhrer, E. C., Mantzanas, K., Koukoura, Z., Gallagher, M., Williams, P., Flynn, M., and Riedo, M.: Biosphere-atmosphere interactions of ammonia with grasslands: Experimental strategy and results from a new European initiative, Plant Soil, 228, 131–145, 2001.

Takahashi, T., Sutherland, S. C., Sweeney, C., Poisson, A., Metzl, N., Tilbrook, B., Bates, N., Wanninkhof, R., Feely, R. A., Sabine, C., Olafsson, J., and Nojiri, Y.: Global sea-air CO$_2$ flux based on climatological surface ocean pCO(**??**), and seasonal biological and temperature effects, Deep-Sea Res. II Top. Stud. Oceanogr., 49, 1601–1622, 2002.

Takahashi, T., Sutherland, S. C., Wanninkhof, R., Sweeney, C., Feely, R. A., Chipman, D. W., Hales, B., Friederich, G., Chavez, F., Sabine, C., Watson, A., Bakker, D. C. E., Schuster, U., Metzl, N., Yoshikawa-Inoue, H., Ishii, M., Midorikawa, T., Nojiri, Y., K÷rtzinger, A., Steinhoff, T., Hoppema, M., Olafsson, J., Arnason, T. S., Tilbrook, B., Johannessen, T., Olsen, A., Bellerby, R., Wong, C. S., Delille, B., Bates, N. R., and de Baar, H. J. W.: Climatological mean and decadal change in surface ocean pCO$_2$, and net sea-air CO$_2$ flux over the global oceans, Deep Sea Res. Part II: Topical Studies in Oceanography, 56, 554–577, 2009.

Timco, G. W. and Weeks, W. F.: A review of the engineering properties of sea ice, Cold Regions Sci. Technol., 60, 107–129, 2010.

Tison, J. L., Haas, C., Gowing, M. M., Sleewaegen, S., and Bernard, A.: Tank study of physico-chemical controls on gas content and composition during growth of young sea ice, J. Glaciol., 48, 177–191, 2002.

Toggweiler, J. R., Gnanadesikan, A., Carson, S., Murnane, R., and Sarmiento, J. L.: Representation of the carbon cycle in box models and GCMs: 1. Solubility pump, Global Biogeochem. Cy., 17, 1027, doi:10.1029/2001GB001841, 2003.

Wang, K., Liu, C., Zheng, X., Pihlatie, M., Li, B., Haapanala, S., Vesala, T., Liu, H., Wang, Y., Liu, G., and Hu, F.: Comparison between eddy covariance and automatic chamber tech-

niques for measuring net ecosystem exchange of carbon dioxide in cotton and wheat fields, Biogeosciences, 10, 6865–6877, doi:10.5194/bg-10-6865-2013, 2013.

Webb, E. K., Pearman, G. I., and Leuning, R.: Correction of Flux Measurements for Density Effects Due to Heat and Water-Vapor Transfer, Q. J. Roy. Meteorol. Soc., 106, 85–100, 1980.

Yelland, M. and Taylor, P. K.: Wind stress measurements from the open ocean, J. Phys. Oceanogr., 26, 541–558, 1996.

Zemmelink, H. J., Delille, B., Tison, J. L., Hintsa, E. J., Houghton, L., and Dacey, J. W. H.: CO_2 deposition over the multi-year ice of the western Weddell Sea, Geophys. Res. Lett., 33, L13606, doi:10.1029/2006GL026320, 2006.